

Neutron diffraction study, magnetic properties and thermal stability of YMn_2D_6 synthesized under high deuterium pressure

V. Paul-Boncour^{a,*}, S.M. Filipek^b, M. Dorogova^b, F. Bourée^c, G. André^c, I. Marchuk^b,
A. Percheron-Guégan^a, R.S. Liu^d

^aLaboratoire de Chimie Métallurgique des Terres Rares, CNRS, 2-8 rue Henri Dunant, 94320 Thiais Cedex, France

^bInstitute of Polish Chemistry, PAN, UL. Kasprzaka 44/52, 01224 Warsaw, Poland

^cLaboratoire Léon Brillouin, CEA-CNRS, CEA/Saclay, 91191 Gif-sur-Yvette, France

^dDepartment of Chemistry, National Taiwan University, Taipei 106, Taiwan, ROC

Received 23 April 2004; accepted 28 May 2004

Abstract

A new phase YMn_2D_6 was synthesized by submitting YMn_2 to 1.7 kbar deuterium pressure at 473 K. According to X-ray and neutron powder diffraction experiments, YMn_2D_6 crystallizes in the $Fm\bar{3}m$ space group with $a = 6.709(1)$ Å at 300 K. The Y and half of the Mn atoms occupy statistically the $8c$ site whereas the other Mn atoms are located in $4a$ site and surrounded by 6 D atoms ($24e$). This corresponds to a K_2PtCl_6 -type structure with a partially disordered substructure which can be written as $[YMn]MnH_6$. No ordered magnetic moment is observed in the NPD patterns and the magnetization measurements display a paramagnetic behavior. The study of the thermal stability by Differential Scanning Calorimetry and XRD experiments indicates that this phase decomposes in YD_2 and Mn at 625 K, and is more stable than $YMn_2H_{4.5}$.

© 2004 Elsevier Inc. All rights reserved.

Keywords: Laves phase; Hydride; High pressure; X-ray diffraction; Neutron diffraction; Magnetism; Differential thermal calorimetry; Thermal stability

1. Introduction

Treatment of metals and alloys by using high hydrogen/deuterium pressure proved to be effective in the syntheses of new hydrides or deuterides. It has been used for binary hydrides like NiH [1] and nickel alloys [2,3], MnH_x [4], FeH_x [5]. More details can be found in several monographs [6–8]. With few exceptions (MnH_x can be given as example) the hydrides formed at high hydrogen pressure are not stable at normal conditions. We expected that the application of high hydrogen pressure to RT_2 (R = rare-earth and T = transition metal intermetallic compounds) may extend the hydrogen absorption to higher values with formation of new

crystalline phases remaining stable at normal conditions.

As expected, we succeeded to form and study new hydrides (deuterides) of Laves-phase compounds like $ZrCo_2H_2$ and $ZrFe_2H_{3.6}$ [9,10], YFe_2H_5 and $ErFe_2H_5$ [11,12] and more recently YMn_2H_6 [13]. The hydrogen content stored in YMn_2H_6 corresponds to a weight capacity of 3% which is the largest value for such compound and is comparable to what is obtained in ZrV_2H_6 for example [14].

The previous X-ray diffraction (XRD) analysis has shown that YMn_2H_6 crystallizes in a face-centered cubic structure ($a = 6.707$ Å) [13]. This structure is quite different from that observed for the already known YMn_2H_x hydrides (deuterides) ($0 < x \leq 4.5$) which retains a structure derived from the cubic $MgCu_2$ type structure of YMn_2 . At room temperature these hydrides show an increase of the cubic cell parameter up to

*Corresponding author. Fax: +33 1 49 78 12 03.

E-mail address: paulbon@glvt-cnrs.fr (V. Paul-Boncour).

$x = 3.5$ and a rhombohedral distortion for $4 \leq x \leq 4.5$ [15–20]. In contrast to these rather small distortions it seems that the crystal structure of YMn_2H_6 results from a complete reorganization of the unit cell of the parent compound, but to check this assumption it is necessary to determine also the location of the H atoms. For this purpose we have investigated the crystal structure of YMn_2D_6 using neutron powder diffraction (NPD) experiments. The magnetic structure was also studied by the NPD analysis and magnetic measurements. In order to determine the thermal stability of YMn_2D_6 we used the Differential Scanning Calorimetry (DSC) measurements and sample characterization by XRD after various heat treatments. These results are presented in this paper and discussed in relation with the properties of the $\text{YMn}_2\text{H}_{4.5}$ hydride.

2. Experimental

YMn_2 was prepared by induction melting of the pure elements (Y, 99.9% from Santoku America and Mn 99.99% from alpha products) followed by an annealing treatment of 11 days at 1073 K. The homogeneity of the sample was checked by XRD and electron microprobe analysis (EPMA). The intermetallic sample was single phase with a cubic C15 structure and $a = 7.681(1)$ Å. About 6 g of YMn_2D_6 has been prepared for the neutron diffraction experiments under 1.7 kbar deuterium pressure and 473 K [13]. The $\text{YMn}_2\text{H}_{4.5}$ hydride was synthesized as in Ref. [20]. After deuteration the powder remains black and the sample is stable under air during several months.

Density measurements have been performed using a volumetric method with an Accupyc 1330 Picnometer from Micromeritics Company.

The XRD patterns were measured with a D8 Bruker diffractometer equipped with a rear graphite monochromator in the range $10^\circ < 2\theta < 120^\circ$ with a step of 0.02° using $\text{CuK}\alpha$ radiation. The samples were deposited on a flat plate with 0.2 mm thickness.

The NPD patterns of the deuteride have been registered at 2 and 80 K on the 3T2 diffractometer and at 1.5, 80 and 290 K on the G4.1 diffractometer at the Laboratoire Léon Brillouin (LLB) at Saclay. For the 3T2 experiment the wavelength was 1.225 Å and the angular range $6^\circ < 2\theta < 125^\circ$ with a step of 0.05° . For the G4.1 experiments the wavelength was 2.427 Å and the angular range was $2^\circ < 2\theta < 82^\circ$ with a step of 0.1° . The deuteride sample was contained in a vanadium tube of 8 mm diameter. All the XRD and NPD patterns were refined with the Rietveld method, using the Fullprof code [21]. The line shapes were refined with a Pearson VII function.

DSC was performed on TA-Q100 DSC apparatus from TA Instrument. The samples were placed in

aluminum pans under flowing purified argon atmosphere. The experiments were performed from 313 K up to temperatures ranging from 523 to 750 K with a rate of 20 K/min.

Magnetization measurements were performed from 5 to 290 K on a Quantum Design PPMS magnetometer with applied field up to 5 T.

3. Results and discussion

3.1. Structure

Density measurements led to a value of $d = 4.63(1)$ g/cm³. This experimental density is in good agreement with the calculated one: $d = 4.636$ g/cm³ for YMn_2D_6 in a fcc cell with $a = 6.709$ Å and $Z = 4$.

The G4.1 experiments performed at various temperatures, between 1.5 and 290 K, revealed very few changes in the NPD patterns: a small increase of the background as the temperature increases and a shift of the peaks due to the increase of the cell parameter.

To solve the nuclear structure we have analyzed the NPD pattern measured at 2 K on 3T2. In a previous work [13] the XRD pattern of YMn_2D_6 was refined in a cubic structure described in the $F\bar{4}3m$ space group where the Y is on the $4a$ site and the Mn on $4b$ and $4c$ sites. Using this space group description, a Fourier difference of the experimental and calculated NPD pattern indicated that the D atoms should occupy the $24g$ position with x close to 0. Nevertheless this solution led to very bad refinement of the NPD pattern with an R_{Bragg} of 43%. The Fourier difference analysis revealed that no other sites were occupied but that the density was too large or too small on the $4a$ and $4b$ sites depending on whether it was occupied by Y or Mn atoms. A good refinement ($R_{\text{Bragg}} = 6.3\%$) was obtained with a statistical occupation of Y and Mn atoms in the $4a$ and $4b$ positions. This structure can be also described in the $Fm\bar{3}m$ space group (supergroup of $F\bar{4}3m$) corresponding to the crystal structure (K_2PtCl_6 type structure) of Mg_2FeH_6 [22] and other isostructural $M_2\text{TH}_6$ hydrides [23,24], where M and T represent two different metals. In Mg_2FeH_6 the Mg atoms occupy the $8c$ site, Fe the $4a$ site and D atoms the $24e$ site. But as determined previously, the NPD pattern could not be refined in an ordered structure (for example Mn on $8c$ and Y on $4e$ sites led to an R_{Bragg} of 120%). The only solution to refine correctly the NPD line intensities was to assume a statistical occupancy of the $8c$ site by 4 Y and 4 Mn (Mn1) atoms, whereas the $4a$ site is occupied by 4 other Mn (Mn2) atoms and the $24e$ site by the D atoms (Table 1). This crystal structure led also to a better refinement of the XRD pattern at 300 K ($R_{\text{Bragg}} = 5.81\%$) than in the ordered structure described in the $F\bar{4}3m$ space group ($R_{\text{Bragg}} = 8\%$) [13].

Table 1

Unit cell parameter (a), cell volume (V), wave length (λ), refined atomic positions (x), occupation numbers (N), Debye–Waller factor (B), line width parameters (U, V, W, Y) and reliability factors ($R_1, R_{wp}, R_{exp}, \chi^2$) for YMn_2D_6 NPD pattern measured on 3T2 at 2 K. Total number of independent reflections: 48

Space group	$Fm\bar{3}m$	$a = 6.6894(1) \text{ \AA}$	$V = 299.34(1) \text{ \AA}^3$	$\lambda = 1.225 \text{ \AA}$
Atoms	Wyckoff position	x	N	$B (\text{Å}^2)$
Y	8c		0.49(1)	0.09(4)
Mn1	8c		0.51(1)	0.00(4)
Mn2	4a		1	0.00(4)
D	24e	0.2465(3)	1	1.50(2)
$U = 1.48(2)$	$V = -0.50$	$W = 0.25$	$Y = 0.12(1)$	
$R_{Bragg} = 7.1\%$		$R_{wp} = 5.0\%$		
$R_{exp} = 2.2\%$		$\chi^2 = 5.1$		

Weak additional lines due to few percent (5.8%) of rhombohedral deuteride $YMn_2H_{4.5}$ and Y_2O_3 (2.5%) were observed in the XRD pattern. Very small additional lines were also observed in the NPD pattern, but much weaker than in the XRD pattern since the neutron have a larger penetration length than the X-ray, and are therefore less sensitive to the surface. The 3T2 NPD (2 K) pattern refined as described in Table 1 is reported in Fig. 1. The refinement of the 3T2 NPD pattern at 80 K leads to the same structure as that at 2 K with only a small increase of the cell parameter ($a = 6.6894(1) \text{ \AA}$ at 2 K and $a = 6.6909(1) \text{ \AA}$ at 80 K). The NPD patterns of YMn_2D_6 measured on G4.1 diffractometer (devoted to the study of magnetic structure) contains weak additional reflections at low angles, which cannot be refined in the fcc cubic cell of YMn_2D_6 . However, all of them can be refined with the nuclear (3%) and magnetic structure of rhombohedral $YMn_2D_{4.5}$ (Fig. 2) [16,25].

Fig. 3 shows a schematic representation of the cubic structure of YMn_2D_6 described in the $Fm\bar{3}m$ space group. The coordination numbers and the calculated interatomic distances of the first neighbors are reported in Table 2.

The random (Y, Mn) substitution on the 8c site is rather surprising if we consider the difference between the metallic atomic radius of Y (1.80 Å) and Mn (1.40 Å) atoms. However, this difference is reduced if instead of metallic radii the covalent radii are considered Y (1.62 Å) and Mn (1.39 Å). In addition the small bump observed around $d = 4.74 \text{ \AA}$ in both 3T2 and G4.1 NPD patterns can indicate a short range order, which correspond to the distance between two Y(Mn1) or two Mn2 atoms. Since no short range order between two Mn2 atoms is expected, it can rather be related to the existence of a short range order of Y and Mn atoms on the 8c site.

Another important feature is that the deuterium atoms are not located into interstitial sites (A2B2 or AB3) like in other YMn_2H_x hydrides but form octahedra around the Mn2 atoms. The distances between the D atoms ($d = 2.34 \text{ \AA}$) are larger than the

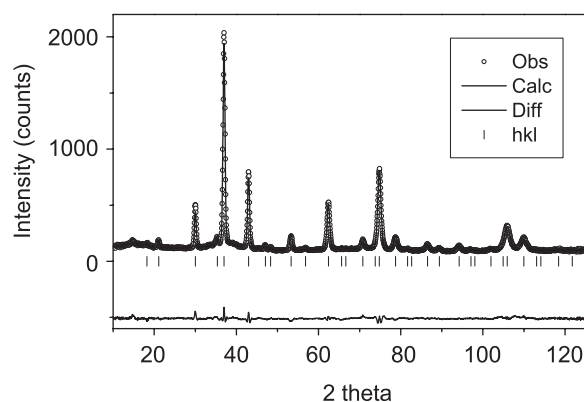


Fig. 1. Experimental and refined NPD pattern of YMn_2D_6 measured on 3T2 at 2 K.

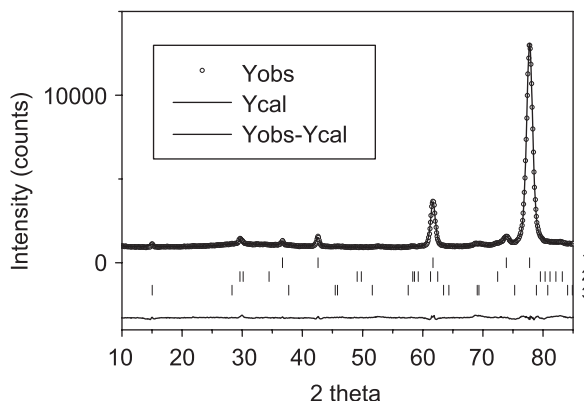


Fig. 2. NPD pattern of YMn_2D_6 measured on G41 at 1.5 K. The tick correspond to the (hkl) of (1) YMn_2D_6 , (2) nuclear and (3) magnetic structure of $YMn_2D_{4.5}$.

Switendik criterium $d = 2.1 \text{ \AA}$ [26], whereas the Mn2–D distances (1.65 Å) are shorter than the sum of the atomic metallic radius (1.75 Å). A comparison with $YMn_2D_{4.5}$ which crystallizes in the rhombohedral $R\bar{3}m$ space group with 2 Y sites, 2 Mn sites and 3 D sites [16,25] also indicates a change of bonding type. In $YMn_2D_{4.5}$ each Mn atom is surrounded by 6 Mn at 2.89–2.92 Å whereas

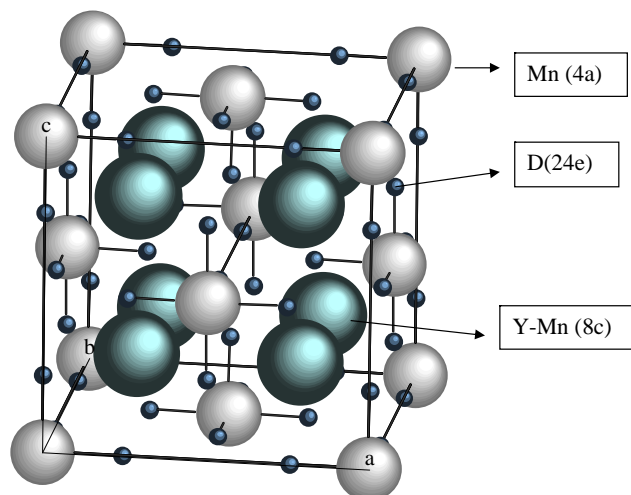
Fig. 3. Schema of the cubic structure of YMn_2D_6 .

Table 2

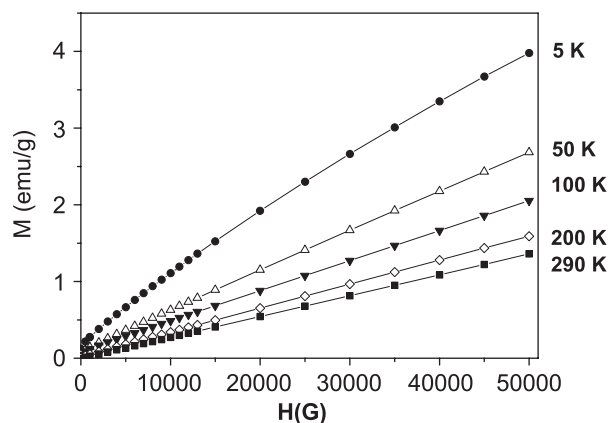
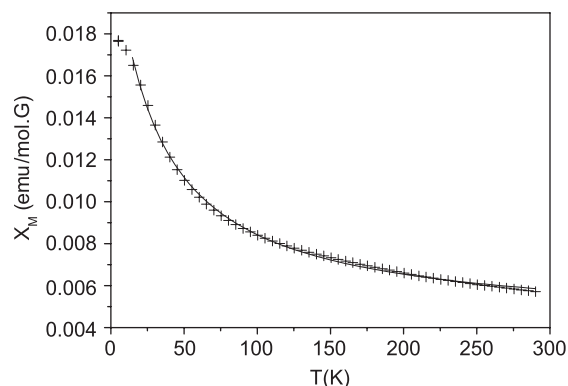
Coordination numbers and interatomic distances in YMn_2D_6 calculated with $a = 6.709(1) \text{ \AA}$ measured at 300 K

Atom neighbor central	Y–Mn1 (Å)	Mn2 (Å)	D (Å)
Y–Mn1 (8c)	6–3.355(1) 12–4.744(1)	4–2.905(1)	12–2.372(1)
Mn2 (4a)	8–2.905(1)	12–4.744(1)	6–1.654(7)
D (24e)	4–2.372(1)	1–1.654(7)	4–2.339(10)

in YMn_2D_6 , taking into account the half occupancy of the 8c site, each Mn is surrounded by 4 Mn at 2.90 Å. This means that if the Mn–Mn interatomic distances are conserved, the Mn coordination numbers changes significantly. The distances between the Y and Mn atoms in $\text{YMn}_2\text{D}_{4.5}$ varies between 3.39 and 3.43 Å which is large compared to 2.905 Å in YMn_2D_6 . This confirms a significant change in the nature of the bonding between Y and Mn atoms.

In $\text{YMn}_2\text{D}_{4.5}$ the Mn–D distances varies between 1.77 and 1.92 Å and the Y–D distance between 2.188 and 2.386 Å. These distances are larger than the Mn2–D distances (1.654 Å) observed in YMn_2D_6 and also suggest a different type of Mn–D bonding.

This raises the question if the magnetic order in YMn_2D_6 . $\text{YMn}_2\text{D}_{4.5}$ is antiferromagnetic with a moment of $3.2 \mu\text{B}$ by Mn atoms at 1.5 K and a Néel temperature of 330 K [25]. The analysis of the NPD patterns of YMn_2D_6 from 1.5 to 290 K has revealed that there is no long-range ordered magnetic structure associated with this phase. The magnetization curves display a linear behavior down to 50 K and should be related to a paramagnetic behavior (Fig. 4). At 5 K there is a weak ferromagnetic component, which can be attributed to small amount of secondary phases or impurities. The inverse of the magnetic susceptibility is

Fig. 4. Magnetization curves of YMn_2D_6 at various temperatures.Fig. 5. Evolution of the molar susceptibility of YMn_2D_6 (+) and refinement (line) with a Pauli paramagnet constant susceptibility and a Curie–Weiss law.

not linear versus temperature indicating that this evolution is not related to a simple Curie–Weiss law. However, it is possible to refine (Fig. 5) the magnetic molar susceptibility χ_M with the sum of a Pauli paramagnet temperature independent susceptibility and a Curie–Weiss law:

$$\chi_M = \chi_0 + \frac{C}{T - \theta_p} \quad (1)$$

with $\chi_0 = 0.004 \pm 0.001 \text{ emu/mol}$, $C = 0.55 \text{ emu/mol K G}$ and $\theta_p = -30 \text{ K}$. Assuming that the Curie–Weiss law concerns half the Mn atoms this would lead to an effective Mn moment of about $3 \mu_B$ close to that observed in other YMn_2 hydrides. Since the shorter Mn–Mn distances in YMn_2D_6 are similar to those of $\text{YMn}_2\text{D}_{4.5}$ (2.90 Å), one would have expected the existence of an ordered antiferromagnetic or ferrimagnetic structure for YMn_2D_6 . However, due to the strong Mn2–D bonding, the interaction between the Mn1 and Mn2 atoms in YMn_2D_6 should be very different from that observed in $\text{YMn}_2\text{D}_{4.5}$. Goncharenko et al. [27] have shown that the Mn–Mn interactions in $\text{RMn}_2\text{H}_{4.5}$

hydrides are very sensitive to the hydrogen surrounding and could be either ferromagnetic or antiferromagnetic depending of the presence or absence of one H atom between the two Mn atoms. In the case of YMn_2D_6 , the octahedral cage of deuterium atoms seems to prevent any long range order magnetic interaction.

3.2. Thermal stability

Fig. 6 displays the evolution of the DSC signal of $\text{YMn}_2\text{H}_{4.5}$ and YMn_2D_6 up to 673 K. In order to

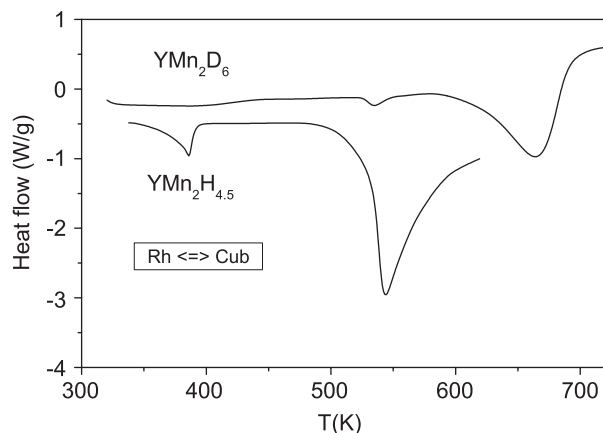


Fig. 6. Evolution of the DSC signal versus temperature for $\text{YMn}_2\text{H}_{4.5}$ and YMn_2D_6 .

identify the origin of these peaks, XRD measurements were performed on $\text{YMn}_2\text{H}_{4.5}$ and YMn_2D_6 after different heating temperatures in the DSC apparatus as summarized in Table 3. The H content in the YMn_2H_x phases was estimated from their cell parameters using the data of Ref. [20].

The endothermic peak observed for $\text{YMn}_2\text{H}_{4.5}$ at 386 K (41.57 J/g) can be attributed to the reversible rhombohedral–cubic transformation according to previous ND measurements [16]. A detailed DSC analysis, with temperature cycles at every 5 K, indicates that this peak intensity progressively decreases as the heating temperature is raised between 445 and 520 K due a loss of hydrogen in $\text{YMn}_2\text{H}_{4.5}$ until complete disappearance of the rhombohedral phase.

A second broad endothermic peak is observed around 540 K for $\text{YMn}_2\text{H}_{4.5}$, with a large enthalpy of reaction ($\Delta H = 190$ J/mol). According to the XRD analysis of $\text{YMn}_2\text{H}_{4.5}$ between 523 and 593 K this peak can be attributed to a fast deuterium desorption from $x = 3.5$ to 1.8 H/f.u. (Table 3). As temperature is higher, slower hydrogen desorption takes place. The XRD analysis indicates that after heating at 643 K there is a partial decomposition of the hydride into YH_2 and Mn, and probably a beginning of amorphization beside a remaining crystalline $\text{YMn}_2\text{H}_{0.1}$ phase.

Concerning YMn_2D_6 a very small peak is also observed at 386 K due to the 2–3% of rhombohedral

Table 3
XRD results for $\text{YMn}_2\text{H}_{4.5}$ and YMn_2D_6 after DSC experiments

T_{\max} (K)	$\text{YMn}_2\text{H}_{4.5}$			YMn_2D_6		
	Phase	%	Cell parameter (Å)	Phase	%	Cell parameter (Å)
298	$\text{YMn}_2\text{H}_{4.5}$	100	$a = 5.860(1)$ $c = 14.07(2)$	YMn_2D_6 $\text{YMn}_2\text{D}_{4.5}$	93 7	$a = 6.709(1)$ $a = 5.860(1)$ $c = 14.07(2)$
493	$\text{YMn}_2\text{H}_{4.5}$ $\text{YMn}_2\text{H}_{3.7}$	95 5	$a = 5.860(1)$ $c = 14.07(1)$ $a = 8.138(1)$			
523	$\text{YMn}_2\text{H}_{3.5}$ $\text{YMn}_2\text{H}_{2.5}$	34 66	$a = 8.113(1)$ $a = 8.013(1)$	YMn_2D_6	100	$a = 6.707(1)$
573	$\text{YMn}_2\text{H}_{2.1}$ $\text{YMn}_2\text{H}_{1.9}$	28 72	$a = 7.975(1)$ $a = 7.952(1)$	YMn_2D_6	100	$a = 6.705(1)$
593	$\text{YMn}_2\text{H}_{1.6}$	100	$a = 7.922(1)$	YMn_2D_6 YD_2	62 38	$a = 6.705(1)$
623	$\text{YMn}_2\text{H}_{1.4}$	100	$a = 7.909(1)$	YMn_2D_6 YD_2 Mn	22 35 42	$a = 6.688(2)$ $a = 5.139(9)$ $a = 8.922(5)$
643	$\text{YMn}_2\text{H}_{0.1}$ YH_2 Mn	10 36 55	$a = 7.727(1)$ $a = 5.147(1)$ $a = 8.890(4)$			
673	YH_2 Mn			YD_2 Mn	44 55	$a = 5.139(9)$ $a = 8.922(5)$

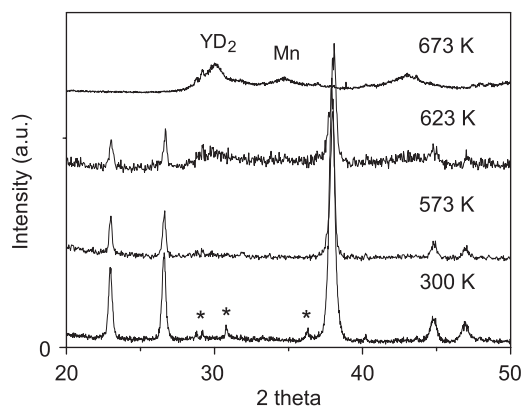


Fig. 7. Evolution of the YMn_2D_6 patterns after various DSC treatments. The temperatures correspond to the DSC experiment maximum temperatures. The stars are related to second phase: rhombohedral and cubic deuteride.

$YMn_2D_{4.5}$. The peak at 540 K can also be attributed to the desorption of the remaining YMn_2D_x phases since this intensity (6 ± 1 J/g) represents only 3% of that observed for $YMn_2H_{4.5}$. This is confirmed by the fact that the lines attributed to $YMn_2D_{4.5}$ have disappeared from the XRD pattern of YMn_2D_6 after heating at 573 K (Fig. 7). The large endothermic peak observed for YMn_2D_6 , which starts at 611 ± 2 K with a maximum at 664 ± 2 K and an enthalpy of 200 ± 2 J/g can be attributed to the deuteride decomposition into YD_2 and α -Mn which is complete at 673 K (Fig. 7). The relative percentage of YD_2 and Mn correspond to a full decomposition and should be accompanied by a desorption of about 4 H/f.u. A weak decrease of the cubic cell parameter of YMn_2D_6 (-0.3%) was observed when increasing the temperature (Table 3) which may imply a very small deuterium desorption.

These results clearly show that YMn_2D_6 displays a larger stability than $YMn_2H_{4.5}$ since its thermal decomposition occurs at higher temperature. The origin of this higher stability can be explained by the fact that the Mn–D bonds are stronger in YMn_2D_6 than in $YMn_2H_{4.5}$. In YMn_2D_6 the Mn–D bonds have a length of 1.65 Å, whereas they are equal or larger than 1.78 Å in $YMn_2H_{4.5}$. In addition in $YMn_2H_{4.5}$ the H atoms are located in interstitial A2B2 tetrahedral sites and H desorption results in the formation of hydrides with lower H content in the same type of structure. In YMn_2D_6 there is a complete reorganization of the metallic framework which is different from that of the starting compound YMn_2 and therefore the simple hydrogen or deuterium desorption is not possible.

3.3. Discussion

This study has shown that YMn_2D_6 synthesized by submitting YMn_2 to very high hydrogen pressure

(1.7 kbar) display a fluorite-type structure with a disordered substructure. Several isostructural hydrides of M_2TH_6 where M is a alkaline earth ($M = Mg, Ca, Sr$) or a divalent rare earth metal ($M = Eu, Yb$) and T a transition metal ($T = Fe, Ru, Os$) have already been obtained by sintering the mixture of metallic powder at moderate temperatures (623–800 K) and hydrogen pressure of 70–130 bars [24]. In these compounds the parent intermetallic compounds does not exist and direct hydrogenation is not possible [24].

However, it is the first time to our knowledge that this type of hydride can be obtained by direct reaction of an intermetallic compound with hydrogen (deuterium). Moreover in YMn_2D_6 the 8c site is not a divalent metal but a result from a random distribution of Y and Mn atoms. This marks also a difference with the quaternary complex hydrides $M_1M_2TH_6$ ($M_1M_2 = CaMg$ and $T = Fe$) where an ordered arrangement of the alkaline metal on the 8c site was found [24].

Concerning the nature of the Mn–D bonds it can be noticed that the Mn–D distances ($d(Mn-D) = 1.65$ Å) are close to those observed in other M_2TH_6 hydrides [24]. For example, in Mg_2FeH_6 , $d(Fe-D) = 1.556$ Å and in Mg_2OsH_6 , $d(Os-D) = 1.682$ Å. These short distances are indicative of covalent bonding [22]. These hydrides can therefore be considered as coordination compounds rather than interstitial metal hydrides. In addition these M_2TH_6 compounds are described as complex anions TH_6^{4-} surrounded by a cage of divalent M^{2+} cations. Assuming the same type of electronic configuration and applying the 18 electrons rule the Mn–D should form $[Mn^ID_6]^{5-}$ octahedral complex [28] whereas the Mn1 on the 8c site should be Mn^{II} , if we consider that the Y atoms are Y^{III} . However the ionic state of the Mn atoms is not supported by the previous X-ray absorption (XAS) measurements on YMn_2D_6 which have shown that the Mn L_{2-3} near edge structure are similar to that of Mn in YMn_2 [13]. The Mn K -edge near edge structure is also close to that observed for $YMn_2H_{4.5}$. Compared to the starting intermetallic YMn_2 , there is a decrease of the prepeak intensity corresponding to a transition from $1s$ state to empty $4p$ states hybridized with the $3d$ conduction band. This prepeak intensity progressively decrease as the H content increases as observed in other RM_2H_x hydrides [29]. These XAS results indicate that the Mn atoms are not in an ionic state since this would induce a significant shift of the Mn K -edge position compared to YMn_2 and the other YMn_2H_x related hydrides. Nevertheless the analysis of the magnetic susceptibility with the sum of a Pauli paramagnet and a Curie–Weiss paramagnet, may indicate different magnetic behavior for the Mn1 and Mn2 atoms, in relation with their very different surrounding. Therefore, band structure calculations will be performed in order to get a better understanding of the electronic structure of YMn_2D_6 . In addition Nuclear Magnetic Resonance of

^{55}Mn is in progress to clarify the nature of the two types of Mn atoms in this new deuteride.

4. Conclusion

In this study, we have shown that YMn_2D_6 crystallizes in a disordered fluorite structure which is close to other hydrides like Mg_2FeH_6 and can be denoted as $[\text{YMn}]\text{MnH}_6$. The Mn atoms occupy two types of sites: half of them are randomly substituted with the Y atoms on the $8c$ site while the other occupy the $4c$ site and are surrounded by 6 deuterium atom at 1.65 \AA . The neutron experiments down to 1.5 K did not reveal any ordered magnetic structure for this compound. The magnetic curves were analyzed assuming a sum of Pauli and Curie–Weiss paramagnetic behavior resulting from two different types of Mn atoms, due to their very different D surrounding. The study of the thermal decomposition of YMn_2D_6 and $\text{YMn}_2\text{H}_{4.5}$ hydrides through DSC and XRD experiments indicate a higher thermal stability for YMn_2D_6 . This can be attributed to the stronger Mn–D bonding and the difference in the structure compared to the C15 one of the parent compound.

Acknowledgments

We are thankful to V. Lalanne for the synthesis of YMn_2 and E. Leroy for the EPMA analysis.

References

- [1] B. Baranowski, R. Wisniewski, *Bull. Acad. Pol. Sci.* 14 (1966) 273.
- [2] S.M. Filipek, B. Baranowski, *Rocz. Chem.* 49 (1975) 1149.
- [3] S.M. Filipek, B. Baranowski, M. Yoneda, *Rocz. Chem.* 51 (1977) 2243.
- [4] M. Krukowski, B. Baranowski, *Rocz. Chem.* 49 (1975) 1183.
- [5] V.E. Antonov, I.T. Belash, E.G. Ponyatovskii, *Ser. Metall.* 16 (1982) 203.
- [6] E.G. Ponyatovskii, V.E. Antonov, I.T. Belash, in: A.M. Prokhorov, A.S. Prokhorov (Eds.), *Problems in Solid State Physics*, Mir Publ., Moscow, 1984, pp. 109–171.
- [7] B. Baranowski, S.M. Filipek, in: B. Baranowski, J.J. Jurczak (Eds.), *High Pressure Chemical Synthesis*, Elsevier Science Publishers, Amsterdam, Oxford, New York, Tokyo, 1989.
- [8] Y. Fukai, in: Y. Fukai (Ed.), *The Metal–Hydrogen System, Basic Bulk Properties*, vol. 21, Springer, Berlin, 1993, pp. 71–119.
- [9] S.M. Filipek, I. Jacob, V. Paul-Boncour, A. Percheron-Guégan, I. Marchuck, D. Mogilyanski, J. Pielaszek, *Pol. J. Chem.* 75 (2001) 1921–1926.
- [10] V. Paul-Boncour, F. Bourée, S.M. Filipek, I. Marchuck, I. Jacob, A. Percheron-Guegan, *J. Alloys Compd.* 356–357 (2003) 69–72.
- [11] V. Paul-Boncour, S.M. Filipek, A. Percheron-Guégan, I. Marchuck, J. Pielaszek, *J. Alloys Compd.* 317–318 (2001) 83–87.
- [12] V. Paul-Boncour, S.M. Filipek, I. Marchuck, G. André, F. Bourée, G. Wiesinger, A. Percheron-Guegan, *J. Phys.* 15 (2003) 4349–4359.
- [13] C.-Y. Wang, V. Paul-Boncour, R.-S. Liu, A. Percheron-Guégan, M. Dorogova, I. Marchuck, T. Hirata, S.M. Filipek, H.-S. Sheu, L.-Y. Jang, J.-M. Chen, H.-D. Yang, *Solid State Commun.* 130 (2004) 815–820.
- [14] J.-J. Didisheim, K. Yvon, G. Fischer, D. Shaltiel, *J. Less-Common Met.* 73 (1980) 355–362.
- [15] M. Latroche, V. Paul-Boncour, J. Przewoznik, A. Percheron-Guégan, F. Bourée-Vigneron, *J. Alloys Compd.* 231 (1995) 99–103.
- [16] M. Latroche, V. Paul-Boncour, A. Percheron-Guégan, F. Bourée-Vigneron, *J. Alloys Compd.* 274 (1998) 59–64.
- [17] M. Latroche, V. Paul-Boncour, A. Percheron-Guégan, F. Bourée-Vigneron, G. André, *Physica B* 276–278 (2000) 666–667.
- [18] H. Figiel, A. Lindbaum, C. Kapusta, E. Gratz, *J. Alloys Compd.* 217 (1995) 157–160.
- [19] V. Paul-Boncour, M. Latroche, A. Percheron-Guégan, *J. Solid State Chem.* 150 (2000) 183–187.
- [20] J. Przewoznik, V. Paul-Boncour, M. Latroche, A. Percheron-Guégan, *J. Alloys Compd.* 225 (1995) 436–439.
- [21] J. Rodríguez-Carvajal, in: *Proceedings of Congr. Int. Union of Crystallography*, 1990, p. 127.
- [22] J.-J. Didisheim, P. Zolliker, K. Yvon, P. Fischer, J. Schefer, M. Gubelmann, A.F. Williams, *Inorg. Chem.* 23 (1984) 1953–1957.
- [23] E. Orgaz, M. Gupta, *J. Phys.* 5 (1993) 6697–6718.
- [24] B. Huang, F. Bonhomme, P. Selvam, K. Yvon, P. Fischer, *J. Less-Common Met.* 171 (1991) 301–311.
- [25] I.N. Goncharenko, I. Mirebeau, A.V. Irodova, E. Suard, *Phys. Rev. B* 56 (1997) 2580–2584.
- [26] A.E. Switendick, *Z. Phys. Chem. N. F.* 117 (1979) 89.
- [27] I.N. Goncharenko, I. Mirebeau, A.V. Irodova, E. Suard, *Phys. Rev. B* 59 (1999) 9324–9331.
- [28] H. Kohlmann, *Encyclopedia of Physical Science and Technology*, Academic Press, New York, 2002, pp. 441–458.
- [29] V. Paul-Boncour, A. Percheron-Guegan, *J. Alloys Compd.* 293–295 (1999) 237–242.